Acta Crystallographica Section B
Structural Science
ISSN 0108-7681

Localized defects in radiation-damaged zircon

Susana Ríos,[a]* Thomas Malcherek,[b]† Ekhard K. H. Salje[a] and Chiara Domeneghetti[b]

[a]Department of Earth Sciences, University of Cambridge, Downing Street, Cambridge CB2 3EQ, England, and [b]CNR-CSCC, Dipartimento di Scienze della Terra, Università di Pavia, Via Ferrata 1, 27100 Pavia, Italy

† Present address: Institüt für Mineralogie, Corrensstrasse 24, 48149 Münster, Germany.

Correspondence e-mail: rios@esc.cam.ac.uk

Received 2 March 2000
Accepted 16 June 2000

The crystal structure of a radiation-damaged natural zircon, $ZrSiO_4$ (α-decay radiation dose is *ca* 1.8×10^{18} α-decay events g^{-1}), has been determined. The anisotropic unit-cell swelling observed in the early stages of the amorphization process (0.17% along the *a* axis and 0.62% along the *c* axis compared with the undamaged material) is a consequence of the anisotropy of the expansion of ZrO_8 polyhedra. Larger anisotropic displacement parameters were found for Zr and O atoms, indicating that the distortion produced by α particle-induced localized defects mainly affects the ZrO_8 unit. The overall shape of SiO_4 tetrahedra remains essentially undistorted, while Si—O bonds are found to lengthen by 0.43%.

1. Introduction

Natural zircon, $ZrSiO_4$, is known to undergo amorphization as a consequence of the α-decay of radioactive impurities such as ^{238}U, ^{235}U, ^{232}Th and their α-decay products (Holland & Gottfried, 1955; Ewing, 1994; Weber *et al.*, 1994, and references therein). Understanding the self-radiation damage observed in natural zircon is therefore of great interest owing to its applicability to the evaluation of the damage mechanism observed in structurally similar ceramic nuclear waste forms (Ewing *et al.*, 1996; Weber *et al.*, 1998). The host phases used for the immobilization of excess weapons plutonium and other radionuclides are required to have long-term chemical durability and be radiation-resistant. Since the amorphization undergone by the crystalline polyphases present in these storage matrices may affect the performance of these materials, natural zircon is a good candidate to be used in the study of this phenomenon.

During amorphization the unit-cell volume in natural zircon expands by a maximum of up to 5% compared with the undamaged material (Holland & Gottfried, 1955; Murakami *et al.*, 1991). In the early stages of amorphization, below the first percolation point (*ca* $< 3 \times 10^{18}$ α-decay events g^{-1}; Salje *et al.*, 1999), the material essentially comprises two phases. The minority phase is formed by the amorphous or aperiodic regions that α-recoil nuclei create. The so-called amorphous cascades are ~50 Å in diameter (Weber *et al.*, 1994) and are embedded in the crystalline matrix: the majority phase.

The crystalline matrix is locally perturbed by the α-particles emitted during the decay of the radioactive impurities. Each α-particle has an energy typically around 4.6 MeV, which is mostly released through ionization processes, and at the end of its path by producing several hundreds of isolated atomic displacements all over the crystalline matrix (Weber *et al.*, 1998, and references therein). Monte Carlo calculations on

Table 1
Chemical composition of zircon 269 (Ríos & Salje, 1999).

	Content (wt %)
Zr	49.2 (2)
Si	14.54 (2)
Hf	1.30 (3)
U	0.11 (1)
Th	–
O	34.85

^{239}Pu-doped zircon give an average of 220 atoms displaced per α-particle (Weber *et al.*, 1998). These localized defects are known to be responsible for the large unit-cell expansion observed in radiation-damaged materials. The maximum swelling in zircon (at saturation) is *ca* 1.5% along the *a*-axis and 2% along the *c*-axis, as determined by powder X-ray diffraction (Holland & Gottfried, 1955; Murakami *et al.*, 1991). In natural samples, a large fraction of the α-particle-induced defects are likely to anneal over geological periods. This can be observed in natural zircon, for example. The sigmoidal shape of the swelling along the *a* axis contrasts with the more exponential dose dependence of the expansion along the *c* axis (Holland & Gottfried, 1955; Murakami *et al.*, 1991), indicating that preferential relaxation seems to occur in the basal plane for natural zircon. In Pu-doped zircon (Weber, 1993), where there has been no time for recovery processes, the swelling along the *a* and *c* axes follows similar exponential behaviour.

Much attention has been paid to the mechanism of amorphization itself (Weber *et al.*, 1994, and references therein; Wang *et al.*, 1998) and to the way the structure is recovered after annealing at high temperatures (Vance, 1975; Mursic, Vogt, Boysen & Frey, 1992; Ellsworth *et al.*, 1994; McLaren *et al.*, 1994; Farges, 1994; Zhang, Salje, Capitani *et al.*, 2000). In contrast, almost nothing is known about the nature of α-particle-created point defects in zircon. Recent *ab initio* calculations (Crocombette, 1999) show that thermal isolated defects in zircon are very unlikely to occur and that oxygen interstitials are the only ones having a non-negligible concentration at equilibrium. As far as we are aware, no simulations have been performed for isolated defects induced by α-decay in zircon. The purpose of our present work is to characterize the structural changes induced in the crystalline matrix by the α-particle-created defects and to relate them to the unit-cell swelling observed in natural zircon.

2. Experimental

2.1. Sample

Zircon 269 is originally from Sri Lanka (age 570 ± 20 million years), with uranium as the major radioactive impurity (see chemical composition in Table 1). Electron microprobe analysis showed the uranium to be homogeneously distributed across the sample, within experimental accuracy. No other impurities such as Fe, Ca, Al or Y were found in this sample and the Pb content was found to be less than 0.01 wt%. From the uranium content the radiation dose is estimated to be around 1.8×10^{18} α-decay events g^{-1}. For this radiation dose, diffraction maxima are expected to be a factor of two weaker than in undamaged zircon (Murakami *et al.*, 1986; Weber, 1993). The fraction of aperiodic or amorphous material in this sample is known to be approximately 15% (Ríos *et al.*, 2000).

Table 2
Experimental details.

Crystal data	
Chemical formula	$Zr_{0.99}Hf_{0.01}SiO_4$
Chemical formula weight	184.43
Cell setting	Tetragonal
Space group	$I4_1/amd$
a (Å)	6.618 (3)
c (Å)	6.019 (3)
V (Å^3)	263.58 (19)
Z	4
D_x (Mg m^{-3}) (for the undamaged crystal)	4.648
Radiation type	Mo $K\alpha$
Wavelength (Å)	0.71073
No. of reflections for cell parameters	60
θ range (°)	2–50
μ (mm^{-1})	4.421
Temperature (K)	293 (2)
Crystal volume (mm^3)	0.03
Crystal colour	Colourless
Data collection	
Diffractometer	Philips PW1100
Monochromator	Graphite
$(\sin\theta/\lambda)_{max}$ (Å^{-1})	1.08
Data collection method	ω–2θ scans
Absorption correction	Empirical
No. of measured reflections	2659
No. of independent reflections	382
No. of observed reflections	373
Criterion for observed reflections	$I > 2\sigma(I)$
R_{int}	0.0243
θ_{max} (°)	50.22
Range of h, k, l	$-14 \rightarrow h \rightarrow 14$ $-14 \rightarrow k \rightarrow 14$ $0 \rightarrow l \rightarrow 12$
No. of standard reflections	3
Frequency of standard reflections	Every 400 reflections
Refinement	
Refinement on	F^2
$R[F^2>2\sigma(F^2)]$	0.016
$wR(F^2)$	0.039
S	1.20
No. of reflections used in refinement	382
No. of parameters used	12
H-atom treatment	Mixed
Weighting scheme	$w = 1/[\sigma^2(F_o^2) + (0.025P)^2 + 0.036P]$, where $P = (F_o^2 + 2F_c^2)/3$
$(\Delta/\sigma)_{max}$	0.000
$\Delta\rho_{max}$ (e Å^{-3})	1.101
$\Delta\rho_{min}$ (e Å^{-3})	−1.010
Extinction method	*SHELXL*97 (Sheldrick, 1997)
Extinction coefficient	0.023 (3)
Source of atomic scattering factors	*International Tables for Crystallography* (1992, Vol. C, Tables 4.2.6.8 and 6.1.1.4)
Computer programs	
Structure solution	*SHELXS* (Sheldrick, 1990)
Structure refinement	*SHELXL*97 (Sheldrick, 1997)

Table 3
Room-temperature fractional atomic parameters and anisotropic displacement parameters (Å^2) for zircon 269.

	Zr	Si	O
x	0	0	0
y	0.7500	0.7500	0.06580 (8)
z	0.1250	0.6250	0.19545 (8)
U^{11}	0.00600 (6)	0.00644 (10)	0.01292 (18)
U^{22}	0.00600 (6)	0.00644 (10)	0.00716 (15)
U^{33}	0.00566 (7)	0.00382 (14)	0.00690 (14)
U^{23}	0	0	−0.00100 (12)
U^{13}	0	0	0
U^{12}	0	0	0

This sample was chosen for its relatively low degree of damage. Higher degrees of damage, and therefore broader diffraction maxima, would render the data collection almost unfeasible, whereas for lower degrees of damage the number of defects would be too low and thus their effect too small to be properly analyzed.

2.2. Data collection

Data collection was carried out in a Philips PW1100 four-circle diffractometer with monochromatic Mo $K\alpha$ radiation, using an irregularly shaped fragment of zircon. Radiation damage of the crystal was indicated by significant broadening of the intensity maxima. The intensity data were corrected for absorption using an empirical correction. A summary of the crystal data and data collection parameters is given in Table 2.[1]

2.3. Refinement

The refinement was carried out using the *SHELXL*97 program package (Sheldrick, 1997). Weakly damaged zircon does not show any symmetry change in relation to undamaged zircon, as reported by a previous Raman spectroscopic study (Zhang, Salje, Farnan *et al.*, 2000). Moreover, *hhl* reflections were checked and no violation of the extinction rules was found. Therefore, the structural parameters of undamaged zircon ($I4_1/amd$, $Z = 4$; Robinson *et al.*, 1971) were used as starting parameters for the least-squares refinement. The $\sum w(|F_o|^2 - |F_c|^2)^2$ function was minimized, with w given in Table 2. Scattering factors were chosen according to an effective charge distribution of $(Zr, Hf)^{4+}SiO_4^{4-}$. Hafnium is known to occupy the zirconium site in zircon (Speer & Cooper, 1982) and it was thus included in the structure refinement with a relative occupancy of 0.013. Several strong reflections, for example {020}, {040}, {060}, {132}, {112}, {301} and {312}, showed a large discrepancy with their equivalents owing to anisotropic extinction. Refinement of the anisotropic Becker & Coppens (1974) extinction correction of type I, utilizing the program *PROMETHEUS* (Zucker *et al.*, 1983), yielded extinction correction factors between 0.35 and 0.75 for the above reflections. Anisotropic secondary extinction in radiation-damaged zircon may be expected to arise from the enhanced mosaic spread created by the shear deformation originating from α-particle-induced defects, which is slightly larger in the *ab* plane than along the [001] direction (Ríos & Salje, 1999). For this reason, the above-mentioned reflections were not used in the structure refinement. Positional and anisotropic harmonic mean-square displacement parameters were refined, together with an overall scale factor. Zirconium and hafnium ions were constrained to have identical anisotropic displacement parameters. In the last cycles of the refinement an isotropic extinction coefficient was refined. Real and imaginary parts of the anomalous scattering correction were included in the structure factor calculation. Final positional and displacement parameters are given in Table 3.

[1] Supplementary data for this paper are available from the IUCr electronic archives (Reference: BM0029). Services for accessing these data are described at the back of the journal.

3. Results

The anisotropic unit-cell swelling of zircon 269 is evident when comparing the cell parameters (see Table 2) with those of an undamaged reference zircon with $a = 6.607\,(1)$ and $c = 5.982\,(1)$ Å (Robinson *et al.*, 1971). The a axis expands by $\Delta a/a = 0.17\,(5)\%$, while the swelling along the c axis is almost four times larger, $\Delta c/c = 0.62\,(5)\%$. From the expansion of the cell parameters of Sri Lanka zircons as a function of radiation dose (Holland & Gottfried, 1955; Murakami *et al.*, 1991), we see that the cell parameters obtained for zircon 269 are in reasonable agreement with the radiation dose previously determined.

Crystalline zircon is known to be composed of two distinct polyhedra units: ZrO_8 units are linked by edge-sharing in the basal plane and are connected by edge-sharing to SiO_4 tetrahedra along the c axis (Robinson *et al.*, 1971; see Fig. 1). The polyhedron formed around the central zirconium by the eight closest O atoms is a dodecadeltahedron, which can be visualized as two interpenetrating tetrahedra (Nyman *et al.*, 1984): one of these being elongated, ZrO_4^e, is formed by Zr and

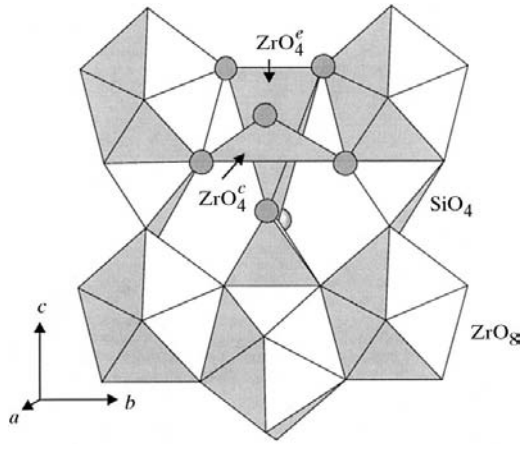

Figure 1
View of the *bc* plane in zircon showing the two interpenetrating ZrO_4 tetrahedra: ZrO_4^e elongated and ZrO_4^c compressed which constitute the ZrO_8 polyhedron.

Table 4
Selected geometric parameters (Å, °) for zircon 269 and undamaged zircon (Robinson *et al.*, 1971).

In the third column we report the expansion/compression of the geometric parameters of zircon 269 in relation to those of undamaged zircon.

	Zircon 269	Undamaged zircon	Relative swelling (%)
SiO_4 tetrahedron			
$Si-O^{i}$	1.6290 (7)	1.622 (1)	0.43 (7)
$O^{ii}-Si-O^{iii}$	96.89 (5)	97.0 (1)	−0.1 (1)
$O^{ii}-Si-O^{i}$	116.11 (3)	116.06 (8)	0.04 (7)
ZrO_8 dodecadeltahedron			
$Zr-O^{iv}$	2.1324 (9)	2.131 (1)	0.07 (6)
$Zr-O^{i}$	2.2816 (9)	2.268 (1)	0.60 (6)
$Zr\cdots Si$	3.0093 (14)	2.991 (2)	0.61 (8)
$Zr\cdots Si^{v}$	3.6349 (12)	3.626 (2)	0.24 (6)
$Zr\cdots Zr^{v}$	3.6349 (12)	3.626 (2)	0.24 (6)
$Si\cdots Si^{ii}$	3.6349 (12)	3.626 (2)	0.24 (6)

Symmetry codes: (i) $y-\frac{1}{4}, x+\frac{3}{4}, z+\frac{1}{4}$; (ii) $-x, -y+1, -z+1$; (iii) $-x, y+\frac{1}{2}, -z+1$; (iv) $x, y+1, z$; (v) $-x+\frac{1}{2}, y, -z+\frac{1}{2}$.

the four O atoms equivalent by symmetry to O^{i}; the other one is compressed, ZrO_4^c, being formed by Zr and the four oxygen atoms equivalent by symmetry to O^{iv} (see Fig. 1). While ZrO_4^e tetrahedra link by edge-sharing to SiO_4 tetrahedra, ZrO_4^c tetrahedra are connected to SiO_4 tetrahedra only *via* corner-sharing. This explains why zircon is *softer* along the *a* axis than along the *c* axis (Özkan *et al.*, 1974).

The most important features helping to clarify the structural changes involved in weakly damaged zircon are the bond lengths and angles. In zircon 269, the observed Zr—O bond length in ZrO_4^e tetrahedra is ∼0.60 (6)% longer than that in undamaged zircon, whereas there is hardly any change [about 0.07 (6)%] for the Zr—O bond length in ZrO_4^c tetrahedra (see Table 4). As ZrO_4^e is elongated along the *c* axis, while ZrO_4^c is compressed in the *ab* plane, the resulting expansion of ZrO_8 units in radiation-damaged zircon is found to be mainly along the *c* axis.

A similar analysis is possible for SiO_4 units. SiO_4 is known to be elongated along the [001] direction in undamaged zircon, as evidenced by the two different O—Si—O bond angles of 116.06 and 97.0°. This elongation has been related to the Zr–Si repulsion (Robinson *et al.*, 1971). In zircon 269, both bond angles remain essentially the same, changing by only 0.04 (7) and 0.1 (1)%, respectively, while the Si—O bonds expand by ∼0.43 (7)%. SiO_4 and ZrO_4^e tetrahedra are thus found to expand in radiation-damaged zircon, in contrast to ZrO_4^c tetrahedra, which do not show any significant change.

Additionally, larger displacement parameters were found in radiation-damaged zircon. From Robinson *et al.*, isotropic temperature factors of undamaged zircon are: U(Zr) = 0.0029 (1), U(Si) = 0.0057 (3) and U(O) = 0.0067 (3) Å^2, whereas in damaged zircon 269, we find 0.00588 (5), 0.00557 (7) and 0.00900 (8) Å^2, respectively. Radiation damage in zircon seems to have more important effects on Zr and O than on Si. Nevertheless, the principal mean displacement parameters for Si of 0.055 (5) and 0.070 (4) Å, along the *a* and *c* axes, respectively, in undamaged zircon, compared to 0.08 (1) and 0.06 (1) Å in zircon 269, indicate that as a consequence of radiation damage, these atoms have larger displacement parameters in the basal plane.

A final difference Fourier map showed no residual peaks which could hypothetically be ascribed to displaced atoms, and we conclude that the main structural difference between weakly radiation-damaged zircon and undamaged zircon is the expansion of ZrO_8 units along the *c* axis, which is accompanied by the expansion of SiO_4 units. The swelling of the *c* axis, by about 0.62% for zircon 269, is in very good agreement with the expansion observed in the Zr···Si distance (parallel to **c**) of 0.61% (see Table 4).

4. Discussion

Localized defects in zircon are most probably interstitial-vacancy pairs related to the large ZrO_8 polyhedra, as it is the less stable unit in zircon (Mursic, Vogt & Frey, 1992). Most of the α-particle-displaced atoms will therefore be Zr and O. Si is expected to be well confined inside rigid SiO_4 units. If we assume that 220 atoms are displaced per α-particle, we expect to find in zircon 269 one Frenkel defect for two unit cells. The strains produced in the neighbourhood of these displaced atoms (mainly Zr and O) are accommodated in the structure by distorting and twisting neighbouring polyhedra. This local rearrangement is the origin of the swelling of the large ZrO_4^e tetrahedra. As ZrO_4^e tetrahedra are strongly linked to SiO_4 units, it is understandable that these units show a similar swelling. This rearrangement of the structure explains the observed unit-cell swelling, as well as of the shear waves found by diffuse X-ray scattering experiments (Ríos & Salje, 1999).

These isolated defects are expected to be randomly distributed through the crystalline matrix. Thus, as we are looking at the average structure, the effect of these defects will only be visible on the anisotropic displacement parameters. As no significant effect was observed on the linking angles, the larger displacement parameters observed in radiation-damaged zircon, in particular for O atoms (see Fig, 2), must account for the relative twisting of neighbouring ZrO_8 and SiO_4 polyhedra.

Although a large fraction of the defects is likely to anneal over geological times, some defects are expected to remain within the structure. As the structure is softer along the *a*(*b*) axis, preferential relaxation along these directions during geologic times might well induce the recovery of the structure in this plane. From Fig. 1 one can see that the structure can reorganize itself more freely by tilting around the corner-sharing links along *a* and *b* axes (*i.e.* the corners between ZrO_4^e and ZrO_4^c polyhedra), releasing the expansion along these directions. Removing the defects produced by expansion along the [001] direction would be more difficult owing to the stronger links between ZrO_4^e and SiO_4 polyhedra. This explains the larger expansion of ZrO_8 polyhedra along the [001] direction. The relaxation in the *ab* plane may as well be

the origin of the larger principal mean displacement parameters of Si. This ability of the structure to recover would explain why no symmetry lowering is observed in weakly damaged natural zircon. All these observations agree with the features of the high-temperature transition at 1100 K found in undamaged zircon (Mursic, Vogt & Frey, 1992). At this transition, with no apparent symmetry change, the expansion of SiO_4 units is accompanied by the expansion of ZrO_4^e tetrahedra, while ZrO_4^c units are accommodated, with almost no bond distance change, by tetrahedra tilting.

For higher degrees of damage, corresponding to higher dosages of α-particles, the recovery along the *a* axis would eventually become more difficult, and the *a* and *c* axes would show similar behaviour, as indicated by the linear relation between *a* and *c* as a function of dose (Holland & Gottfried, 1955; Murakami *et al.*, 1991).

Finally, this rearrangement of the structure and in particular the expansion of the SiO_4 tetrahedron must be responsible for the frequency variation of the stretching Si—O mode observed by Raman spectroscopy in the low dose range ($< 3 \times 10^{18}$ α-decay events g^{-1}; Zhang, Salje, Farnan *et al.*, 2000). In this work, the stretching Si—O mode at 1008 cm^{-1} in undamaged zircon is shown to shift to lower frequencies when increasing the radiation dose. For zircon 269, the relative shift in the mode frequency is estimated to be ~0.8%, which is of the same order of magnitude as the relative unit-cell swelling observed, namely 0.62%.

5. Conclusions

In weakly radiation-damaged zircon, the two interpenetrating tetrahedra that constitute ZrO_8 units are shown to have different behaviour: Zr—O bond lengths in ZrO_4^e tetrahedra expand by 0.60%, whereas no expansion is observed in ZrO_4^c tetrahedra. Consequently, the expansion of ZrO_8 units in radiation-damaged zircon is found to be mainly along the *c* axis. As a consequence of the swelling of the large ZrO_4^e, and due probably to the strong edge-sharing type bonding with SiO_4 units, Si—O bonds swell by ~0.43%. The expansion of SiO_4 tetrahedra explains the frequency variation found for the Si—O stretching mode as a function of radiation dose (Zhang, Salje, Farnan *et al.*, 2000).

The swelling of ZrO_8 units along the [001] direction accounts for most of the unit-cell swelling observed at low levels of radiation damage in zircon. The much smaller expansion in the basal plane is probably a consequence of the annealing along this direction of α-particle-induced point defects over geologic periods. As Pu-doped zircon does not show any relaxation along the *a* axis, it would be interesting to carry out a similar structural study on a sample with a comparable degree of damage, but where no annealing could possibly have occurred.

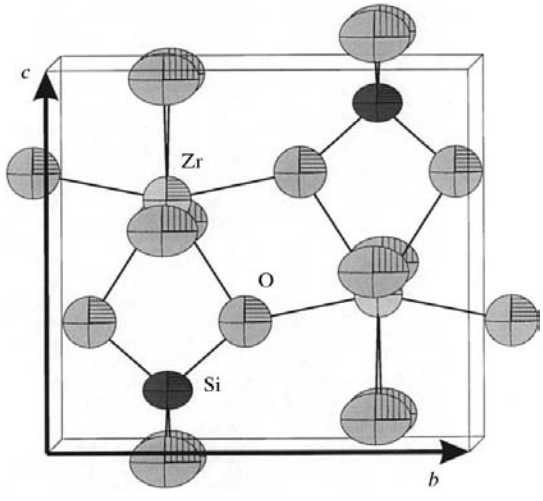

Figure 2
View along the *a* axis of the structure of zircon 269. For clarity, only half of the unit cell has been included and U^{ij} values have been multiplied by 10. The displacement ellipsoids enclose 50% probability. The anisotropy of O atoms is evidence of the disorder present in the structure.

The authors wish to thank the Natural History Museum of London for allowing us to use samples from their collection, in particular sample 269 (BM 1920, 269). This research project was supported by the European TMR Network contract number FMRX-CT97-0108 (DG12-SLJE).

References

Becker, P. J. & Coppens, P. (1974). *Acta Cryst.* A**30**, 129–147.
Crocombette, J. P. (1999). *Phys. Chem. Miner.* **27**, 138–143.
Ellsworth, S., Navrotsky, A. & Ewing, R. C. (1994). *Phys. Chem. Miner.* **21**, 140–149.
Ewing, R. C. (1994). *Nucl. Instrum. Methods Phys. Res. B*, **91**, 22–29.
Ewing, R. C., Weber, W. J. & Lutze, W. (1996). *Disposal of Weapon Plutonium*, edited by E. R. Merz and C. E. Walter, pp. 65–83. Kluwer Academic Publishers.
Farges, F. (1994). *Phys. Chem. Miner.* **20**, 504–514.
Holland, H. D. & Gottfried, D. (1955). *Acta Cryst.* **8**, 291–300.
McLaren, A. C., FitzGerald, J. D. & Williams, I. S. (1994). *Geochim. Cosmochim. Acta*, **58**, 993–1005.
Murakami, T., Chakoumakos, B. C. & Ewing, R. C. (1986). *Adv. Ceram. Nucl. Waste Manage. II*, **20**, 745–753.
Murakami, T., Chakoumakos, B. C., Ewing, R. C., Lumpkin, G. R. & Weber, W. J. (1991). *Am. Mineral.* **76**, 1510–1532.
Mursic, Z., Vogt, T., Boysen, H. & Frey, F. (1992). *J. Appl. Phys.* **25**, 519–523.
Mursic, Z., Vogt, T. & Frey, F. (1992). *Acta Cryst.* B**48**, 584–590.
Nyman, H., Hyde, B. G. & Andersson, S. (1984). *Acta Cryst.* B**40**, 441–447.
Özkan, H., Cartz, L. & Jamieson, J. C. (1974). *J. Appl. Phys.* **45**, 556–562.
Ríos, S. & Salje, E. K. H. (1999). *J. Phys. Condens. Matter*, **11**, 8947–8956.
Ríos, S., Salje, E. K. H., Zhang, M. & Ewing, R. C. (2000). *J. Phys. Condens. Matter*, **12**, 2401–2412.
Robinson, K., Gibbs, G. V. & Ribbe, P. H. (1971). *Am. Mineral.* **56**, 782–790.
Salje, E. K. H., Chrosch, J. & Ewing, R. C. (1999). *Am. Mineral.* **84**, 1107–1116.
Sheldrick, G. M. (1990). *Acta Cryst.* A**46**, 467–473.
Sheldrick, G. M. (1997). *SHELXL*97. University of Göttingen, Germany.

Speer, J. A. & Cooper, B. J. (1982). *Am. Mineral.* **67**, 804–808.
Vance, E. R. (1975). *Radiat. Eff.* **24**, 1–6.
Wang, S. X., Wang, L. M. & Ewing, R. C. (1998). *Mater. Res. Soc. Symp. Proc.* **504**, 165–170.
Weber, W. J. (1993). *J. Am. Ceram. Soc.* **76**, 1729–1738.
Weber, W. J., Ewing, R. C., Catlow, C. R. A., Díaz de la Rubia, T., Hobbs, L. W., Kinoshita, C., Matzke, H., Motta, A. T., Nastasi, M., Salje, E. K. H., Vance, E. R. & Zinkle, S. J. (1998). *J. Mater. Res.* **13**, 1434–1484.
Weber, W. J., Ewing, R. C. & Wang, L. M. (1994). *J. Mater. Res.* **9**, 688–698.
Zhang, M., Salje, E. K. H., Capitani, G. C., Leroux, H., Clark, A. M., Schlüter, J. & Ewing, R.C. (2000). *J. Phys. Condens. Matter*, **12**, 3131–3148.
Zhang, M., Salje, E. K. H., Farnan, I., Graeme-Barber, A., Daniel, P., Ewing, R. C., Clark, A. M. & Leroux, H. (2000*b*). *J. Phys. Condens. Matter*, **12**, 1915–1925.
Zucker, U. H., Perenthaler, E., Kuhs, W. F., Bachmann, R. & Schulz, H. (1983). *J. Appl. Cryst.* **16**, 358–359.